Synthesis and Light-Emitting Properties of Difunctional Dendritic Distyrylstilbenes

Chi Chung Kwok and Man Shing Wong*

Department of Chemistry, The Hong Kong Baptist University, Kowloon Tong, Hong Kong, SAR China

Received May 1, 2001; Revised Manuscript Received July 2, 2001

ABSTRACT: A novel series of poly(benzyl ether) type dendritic distyrylbenzenes bearing various electron or hole affinitive moieties including 1,3,4-oxadiazole, cyano, and propoxy groups on the outer surface of the first- and second-generations dendritic wedges have been synthesized for blue-light emission. Both theoretical and optical studies show that incorporation of the surface functionalized dendritic wedges into the nonconjugated meta positions of a distyrylstilbene skeleton does not disrupt the coplanarity of the π-conjugated core. Excitation of the surface functionalized dendritic wedges leads to substantial energy transfer from the dendritic wedges to the emissive core (up to 59%). Importantly, all the dendritic distyrylstilbenes show very high fluorescence quantum yields (over 93%). Single-layer light-emitting diodes (LED) using dendritic distyrylstilbene (DSB) doped poly(*N*-vinylcarbazole) (PVK) film as an emissive layer with structure of (ITO/DSB:PVK/Al) have been fabricated and investigated. The emission wavelengths and spectral features are very similar among the solution emission, solid-state photoluminescence, and electroluminescence spectra. The device performance of the first-generation dendritic DSB doped single-layer LEDs is generally superior to that of the corresponding second-generation dendrimer based devices. In addition, the propoxy surface functionalized dendritic DSB devices consistently show the best device performance and relative stability among the others.

Introduction

The potential applications of molecular electroluminescent materials for lighting, black light, and full-color flat-panel display have recently attracted considerable attention.[1−3] In the past few years, a great variety of functionalized molecules and polymers have been explored as active components such as light emitting and charge transport layers in organic light emitting diodes (OLED) in order to enhance the luminescence efficiencies and stabilities of the devices.[3−5] Light emission of an OLED originates from the exciton of emissive molecules, generated from the recombination of electrons and holes, injected from the opposite electrodes sandwiched between the functional layer(s). The quantum efficiency of an OLED depends on the photoluminescence efficiency of the emissive molecule and the balance of the injection and transport of holes and electrons. However, organic luminescence materials such as oligo-phenylenevinylenes and poly-phenylenevinylenes generally exhibit better hole injection and transport properties than electrons, which often lead to low device efficiency especially in a single-layer device structure. The general strategies to circumvent this problem are either to use the highly electron affinitive emissive materials,[6] to employ low work function electrodes such as calcium as a cathode, or to insert an electron-conducting/hole-blocking layer between the emissive layer and cathode in multilayer devices.[7]

In addition to polymeric materials, there are considerable interests in developing and investigating novel emissive oligomers or molecules bearing better balanced charge character, favorable processing properties, and stabilities since they can easily be obtained in high purity and fabricated in a thin film.[5,8] Furthermore, investigation of well-defined and monodisperse oligomers can gain an insight into the structural, emissive, and electronic properties of the related polymeric materials.[9] Dendritic macromolecules,[10−16] which can provide a unique architecture to construct or arrange functionalites for desirable functional properties such as a light-harvesting property,[17] have recently drawn interest as a functional material in OLED. The early work focused on the use of the dendrimers for charge transport materials.[18] Recently, an anthracene core bearing phenylacetylene dendritic wedges[19] and a distyrylbenzene core bearing stilbene dendritic wedges[20] have been synthesized and investigated as a functional (single-component) light-emitting material. On the other hand, dendritic macromolecules may potentially be useful as multifunctional emissive materials in OLED if proper charge transport functionalities are incorporated at the periphery of the dendritic wedges. This may result in improving the imbalanced charge character of the organic luminescence materials. Thus, it is of great interest to investigate and understand the influence of various peripheral functionalities and structures of the dendritic wedge on the optical and electronic properties of the emissive dendrimer. Most recently, hole-transporting, emissive dendrimers having triarylamines at the periphery have been synthesized in order to achieve dye isolation for color tuning via dye mixing.[21]

We herein report the synthesis and structure−properties of a novel series of difunctional dendritic distyrylbenzenes (DSB) bearing different electron or hole affinitive groups on the outer surface of poly(benzyl ether) type dendritic wedges, **1**−**8** (Chart 1), for blue-light emission. The ground- and excited-state molecular properties of the first-generation dendritic DSBs were investigated by PM3 semiempirical quantum mechanical calculations in order to understand and correlate the structure−optical properties of these dendrimers. In addition, single-layer OLEDs using dendritic DSB doped poly(*N*-vinylcarbazole) (PVK) film as an emissive layer with structure of (ITO/DSB:PVK/Al) have been fabricated and investigated.

10.1021/ma010749+ CCC: $20.00
Published on Web 08/17/2001

Chart 1

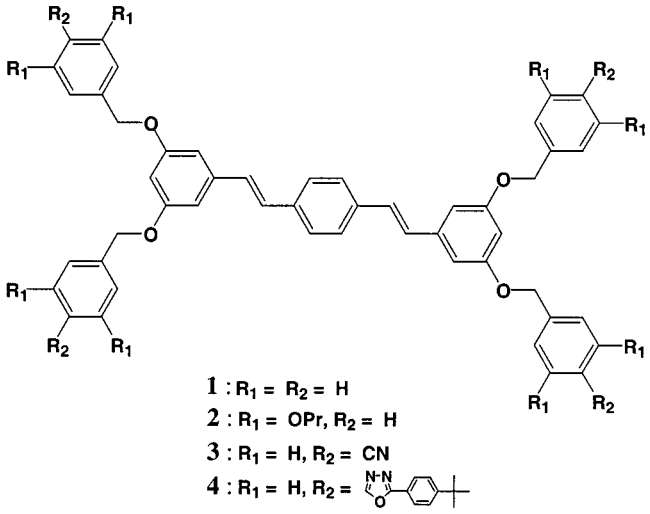

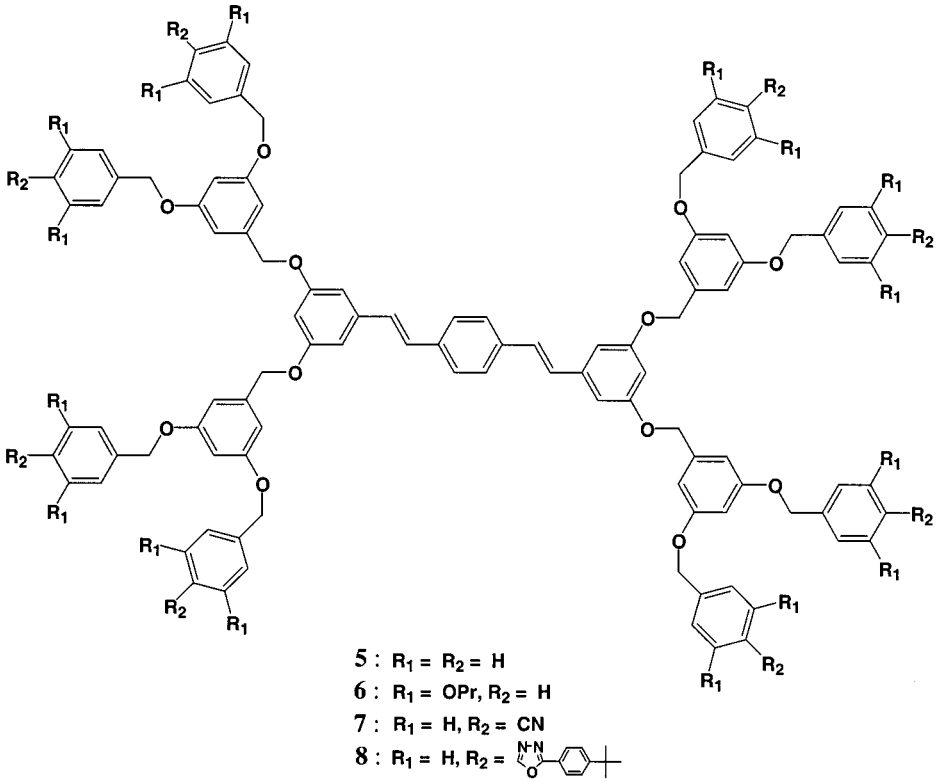

Experimental Section

^{1}H NMR spectra were recorded using a JEOL JHM-EX270 FT NMR spectrometer or a Varian INOVA-400 FT NMR spectrometer and are referenced to the residual $CHCl_3$ 7.24 ppm. ^{13}C NMR spectra were recorded using a Varian INOVA-400 FT NMR spectrometer and are referenced to the $CDCl_3$ 77 ppm. The semiempirical calculations using the PM3 parametrization were carried out by Mopac 6 in the Alchemy 2000 software package. The calculated energy gaps reported in Table 1 were a difference between the HOMO and LUMO levels calculated by Mopac 6. The corrected energy gaps were calculated by adding −1.9 eV for solvent interaction to the calculated energy gaps.[22,23] All the physical measurements were performed in $CHCl_3$. Electronic absorption (UV−vis) and fluorescence spectra were recorded using a Varian Cary 100 scan spectrophotometer and a PTI luminescence spectrophotometer, respectively. The fluorescence quantum yields in chloroform using 9,10-diphenylanthrancene as a standard were determined by the dilution method as described by Parker et al.[24] Thermal stabilities were determined by using a Perkin-Elmer TGA-6 thermal gravimetric analyzer with a heating rate of 10 °C/min.

Table 1. Results of PM3 Semiempirical Calculations of Dendritic DSBs 1-3 and Unsubstituted DSB

	calcd HOMO[b]/eV	calcd LUMO[b]/eV	calcd HOMO−LUMO energy gap/eV	cor calcd energy gap[c]/eV
1	−8.305	−3.359	4.946	3.046
analogue of **2**[a]	−8.215	−3.267	4.948	3.048
3	−8.573	−3.636	4.937	3.037
DSB	−8.329	−3.380	4.949	3.049

[a] Methoxy surface functionalized dendritic DSB. [b] Calculated by PM3 semiempirical quantum mechanical calculations. [c] Corrected with solvent interaction by −1.9 eV (from refs 22 and 23).

Dendritic DSBs doped single-layer OLEDs were fabricated by spin-coating of PVK polymer solution containing 0.133 mmol/g of DSB onto ITO glass substrates. The total solid concentration of polymer solution is 15−19.5 mg/mL in chloroform. The DSB/PVK solution was filtered through a 2 μm PTFE filter, and the ITO glass with a sheet resistance of 80 Ω/m^2 was cleaned with UV−ozone before use. The typical polymer film thickness is about 100 nm. The aluminum cathode was vapor-deposited onto the polymer film. The thickness of the cathode is typically 100 nm. The evaluation of the OLEDs was performed under ambient conditions.

2-(4-*tert*-Butylphenyl)-5-[4-(bromomethyl)phenyl]-1,3,4-oxadiazole was prepared according to the literature procedures.[25]

General Procedure for the Williamson Ether Reaction. To a solution of 1:2 equiv of 3,5-dihydroxylbenzyl alcohol and the corresponding (benzyl) halide in anhydrous acetone was added 2 equiv of potassium carbonate and catalytic amount of 18-crown-6. The reaction mixture was refluxed under N_2 for 24 h. After removal of solvent, the residue was diluted with water and extracted with CH_2Cl_2 twice, dried over anhydrous $MgSO_4$, and evaporated to dryness. The pure product was separated by silica column chromatography.

3,5-Dipropoxybenzyl Alcohol. The above procedure was followed using 1.6 g (11.3 mmol) of 3,5-dihydroxylbenzyl alcohol, 4 g (23.5 mmol) of 1-iodopropane, 4.8 g (35.3 mmol) of potassium carbonate, and 0.1 g of 18-crown-6. The pure product was separated by silica column chromatography using 3:1 CH_2Cl_2/EtOAc as eluent affording 2.3 g (90.7%) of a white solid. ^{1}H NMR (400 MHz, $CDCl_3$): δ 6.49 (d, J = 2.40 Hz, 2H), 6.37 (t, J = 2.40 Hz, 1H), 4.6 (s, 2H), 3.86 (t, J = 6.40 Hz, 4H), 1.82−1.73 (m, 4H), 1.00 (t, J = 7.60 Hz, 6H). ^{13}C NMR (100 MHz, $CDCl_3$): δ 160.2, 143.2, 104.9, 100.3, 69.4, 64.9, 22.4, 10.4. MS (FAB) m/z 224.3 (M^+).

9. The above procedure was followed using 2.19 g (15.7 mmol) of 3,5-dihydroxylbenzyl alcohol and 6.17 g (37.2 mmol) of benzyl bromide. The pure product was separated by silica column chromatography using 1:1 CH_2Cl_2/EtOAc as eluent affording 4.95 g (85%) of a white solid. ^{1}H NMR (270 MHz, $CDCl_3$): δ 7.42−7.30 (m, 10H), 6.61 (d, J = 1.89 Hz, 2H), 6.53 (t, J = 2.16 Hz, 1H), 5.02 (s, 4H), 4.62 (s, 2H).^{13}C NMR (100 MHz, $CDCl_3$): δ 160.1, 143.4, 136.8, 128.6, 128.0, 127.5, 105.7, 101.2, 70.0, 65.2. MS (FAB) m/z 320.3 (M^+).

10. The above procedure was followed using 0.48 g (3.48 mmol) of 3,5-dihydroxylbenzyl alcohol and 2 g (6.96 mmol) of 3,5-dipropoxybenzyl bromide. The pure product was separated by silica column chromatography using 2:1 CH_2Cl_2/EtOAc as eluent affording 1.5 g (77.9%) of a colorless liquid. ^{1}H NMR (400 MHz, $CDCl_3$): δ 6.59 (d, J = 2.00 Hz, 2H), 6.54 (d, J = 2.00 Hz, 4H), 6.52 (t, J = 2.40 Hz, 1H), 6.40 (t, J = 2.40 Hz, 2H), 4.93 (s, 4H), 4.59 (s, 2H), 3.89 (t, J = 6.60 Hz, 8H), 1.84−1.74 (m, 8H), 1.01 (t, J = 7.40 Hz, 12H). ^{13}C NMR (100 MHz, $CDCl_3$): δ 160.4, 160.0, 143.4, 139.0, 105.6, 105.6, 101.2, 100.7, 70.0, 69.5, 65.2, 22.5, 10.5. MS (FAB) m/z 552.5 (M^+).

11. The above procedure was followed using 1.00 g (7.14 mmol) of 3,5-dihydroxylbenzyl alcohol and 2.90 g (14.8 mmol) of α-bromo-*p*-tolunitrile. The pure product was separated by silica column chromatography using 1:1 CH_2Cl_2/EtOAc as eluent affording 2.33 g (84.9%) of a white solid. ^{1}H NMR (270 MHz, $CDCl_3$): δ 7.66 (d, J = 8.10 Hz, 4H), 7.51 (d, J = 8.10 Hz, 4H), 6.61 (d, J = 1.89 Hz, 2H), 6.47 (t, J = 2.03 Hz, 1H), 5.09 (s, 4H), 4.63 (s, 2H). ^{13}C NMR (100 MHz, $CDCl_3$): δ 159.6, 143.9, 142.2, 132.4, 127.5, 118.6, 111.8, 105.8, 101.3, 68.9, 65.0. MS (FAB) m/z 370.2 (M^+).

12. The above procedure was followed using 0.39 g (2.81 mmol) of 3,5-dihydroxylbenzyl alcohol and 2.51 g (6.7 mmol) of 2-(4-*tert*-butylphenyl)-5-[4-(bromomethyl)phenyl]-1,3,4-oxadiazole. The pure product was separated by silica column chromatography using 1:2 CH_2Cl_2/EtOAc as eluent affording 1.42 g (70.1%) of a white solid. ^{1}H NMR (270 MHz, $CDCl_3$): δ 8.14 (d, J = 8.37 Hz, 4H), 8.05 (d, J = 8.37 Hz, 4H), 7.57 (d, J = 8.37 Hz, 4H), 7.54 (d, J = 9.72 Hz, 4H), 6.65 (d, J = 2.16 Hz, 2H), 6.55 (t, J = 2.03 Hz, 1H), 5.13 (s, 4H) 4.65 (s, 2H), 1.36 (s, 18H). ^{13}C NMR (100 MHz, $CDCl_3$): δ 164.7, 164.1, 159.8, 155.4, 143.8, 140.7, 127.7, 127.1, 126.8, 126.1, 123.5, 121.0, 105.8, 101.3, 69.3, 65.1, 35.1, 31.1. MS (FAB) m/z 721.4 (M^+).

13. The above procedure was followed using 0.094 g (0.67 mmol) of 3,5-dihydroxylbenzyl alcohol and 0.53 g (1.41 mmol) of **9-Br**. The pure product was separated by silica column chromatography using 1:1 CH_2Cl_2/EtOAc as eluent affording 0.364 g (69.3%) of a white solid. ^{1}H NMR (400 MHz, $CDCl_3$): δ 7.43−7.31 (m, 20H), 6.68 (d, J = 2.40 Hz, 4H), 6.60 (d, J = 2.40 Hz, 2H), 6.58 (t, J = 2.40 Hz, 2H), 6.53 (t, J = 2.40 Hz, 1H), 5.02 (s, 8H), 4.96 (s, 4H), 4.60 (s, 2H). ^{13}C NMR (100 MHz, $CDCl_3$): δ 160.0, 159.9, 143.5, 139.2, 136.6, 128.5, 127.9, 127.5, 106.2, 105.5, 101.4, 101.1, 69.9, 69.7, 64.9. MS (FAB) m/z 744.5 (M^+).

14. The above procedure was followed using 0.15 g (1.08 mmol) of 3,5-dihydroxylbenzyl alcohol and 1.34 g (2.18 mmol) of **10-Br**. The pure product was separated by silica column chromatography using 1:1 CH_2Cl_2/EtOAc as eluent affording 1.06 g (81.4%) of a colorless liquid. ^{1}H NMR (400 MHz, $CDCl_3$): δ 6.65 (d, J = 2.00 Hz, 4H), 6.58 (d, J = 2.00 Hz, 2H), 6.55 (d, J = 2.00 Hz, 10H), 6.52 (t, J = 2.40 Hz, 1H), 6.40 (t, J = 2.40 Hz, 4H), 4.95 (s, 4H), 4.94 (s, 8H), 4.60 (s, 2H), 3.89 (t, J = 6.60 Hz, 16H), 1.83−1.74 (m, 16H), 1.02 (t, J = 7.60 Hz, 24H). ^{13}C NMR (100 MHz, $CDCl_3$): δ 160.4, 160.0, 160.0, 143.5, 139.2, 138.9, 106.2, 105.7, 105.6, 101.5, 101.1, 100.7, 70.0, 69.9, 69.5, 65.2, 22.5, 10.5. MS (FAB) m/z 1209.2 (M^+).

15. The above procedure was followed using 0.143 g (1.02 mmol) of 3,5-dihydroxylbenzyl alcohol and 0.95 g (2.12 mmol) of **11-Br**. The pure product was separated by silica column chromatography using 1:1 CH_2Cl_2/EtOAc as eluent affording 0.88 g (65.6%) of a white solid. ^{1}H NMR (400 MHz, $CDCl_3$): δ 7.63 (d, J = 8.00 Hz, 8H), 7.49 (d, J = 8.40 Hz, 8H), 6.63 (d, J = 2.00 Hz, 4H), 6.57 (d, J = 2.00 Hz, 2H), 6.50 (t, J = 2.20 Hz, 2H), 6.41 (t, J = 2.20 Hz, 1H), 5.08 (s, 8H), 4.95 (s, 4H), 4.61 (s, 2H). ^{13}C NMR (100 MHz, $CDCl_3$): δ 159.8, 159.6, 143.6, 142.0, 139.7, 132.4, 127.5, 118.6, 111.7, 106.4, 105.6, 101.6, 101.2, 69.6, 68.9, 65.0. MS (FAB) m/z 844.4 (M^+).

16. The above procedure was followed using 0.039 g (0.28 mmol) of 3,5-dihydroxylbenzyl alcohol and 0.469 g (0.60 mmol) of **12-Br**. The pure product was separated by silica column chromatography using 1:3 CH_2Cl_2/EtOAc as eluent affording 0.32 g (71.5%) of a white solid. ^{1}H NMR (400 MHz, $CDCl_3$): δ 8.03 (d, J = 8.40 Hz, 8H), 7.98 (d, J = 8.00 Hz, 8H), 7.49−7.46 (m, 16H), 6.62 (d, J = 2.00 Hz, 4H), 6.59 (d, J = 2.00 Hz, 2H), 6.50−6.49 (m, 2H), 6.44 (bs, 1H), 4.99 (s, 8H), 4.91 (s, 4H), 4.62 (s, 2H), 1.31 (s, 36H). ^{13}C NMR (100 MHz, $CDCl_3$): δ 164.5, 163.9, 159.7, 159.6, 155.3, 144,0, 140.5, 139.6, 127.6, 126.9, 126.6, 125.9, 123.2, 120.7, 106.2, 105.6, 101.5, 100.9, 69.5, 69.1, 64.6, 34,9, 31.0. MS (FAB) m/z 1546 (M^+).

General Procedure for Functionalized Benzyl Bromide Syntheses. To a solution of benzyl alcohol in anhydrous THF or diethyl ether was slowly added 1.1 equiv of PBr_3. After refluxing for 3 h, the reaction mixture was cooled in an ice−water bath, quenched with cooled water, and then extracted with CH_2Cl_2. The organic layer was then washed with Na_2CO_3 solution, dried over anhydrous $MgSO_4$, and evaporated to dryness. The pure product was separated by silica column chromatography.

3,5-Dipropoxybenzyl Bromide. The procedure above was followed using 1.5 g (6.7 mmol) of 3,5-dipropoxybenzyl alcohol and 2 g (7.4 mmol) of PBr_3 in 150 mL of diethyl ether. The pure product was separated by silica column chromatography using 2:1 petroleum ether/CH_2Cl_2 as eluent affording 1.04 g (54.4%) of a pale yellow liquid. ^{1}H NMR (400 MHz, $CDCl_3$): δ 6.51 (d, J = 2.00 Hz, 2H), 6.38 (t, J = 2.00 Hz, 1H), 4.39 (s, 2H), 3.88 (t, J = 6.60 Hz, 4H), 1.83−1.74 (m, 4H), 1.02 (t, J = 7.40 Hz, 6H). ^{13}C NMR (100 MHz, $CDCl_3$): δ 106.3, 139.5, 107.3, 101.3, 69.5, 33.8, 22.5, 10.5. MS (FAB) m/z 287.3 (M^+).

9-Br. The procedure above was followed using 2.79 g (8.73 mmol) of **9** and 2.37 g (8.76 mmol) of PBr_3. The pure product was separated by silica column chromatography using 1:1 petroleum ether/CH_2Cl_2 as eluent affording 3.34 g (96%) of a white solid. ^{1}H NMR (270 MHz, $CDCl_3$): δ 7.42−7.32 (m, 10H), 6.63 (d, J = 2.16 Hz, 2H), 6.54 (t, J = 2.16 Hz, 1H), 5.02 (s, 4H), 4.04 (s, 2H). ^{13}C NMR (100 MHz, $CDCl_3$): δ 159.9, 139.6, 136.5, 128.5, 127.9, 127.4, 108.0, 102.0, 69.9, 33.5. MS (FAB) m/z 383.2 (M^+).

10-Br. The procedure above was followed using 1.99 g (3.6 mmol) of **10** and 0.98 g (3.6 mmol) of PBr_3. The pure product

was separated by silica column chromatography using 2:1 petroleum ether/CH_2Cl_2 as eluent affording 1.33 g (60.4%) of a colorless liquid. ^{1}H NMR (400 MHz, $CDCl_3$): δ 6.61 (d, J = 2.40 Hz, 2H), 6.54 (d, J = 2.40 Hz, 4H), 6.52 (t, J = 2.40 Hz, 1H), 6.40 (t, J = 2.40 Hz, 2H), 4.93 (s, 4H), 4.39 (s, 2H), 3.89 (t, J = 6.60 Hz, 8H), 1.81−1.75 (m, 8H), 1.01 (t, J = 7.40 Hz, 6H). ^{13}C NMR (100 MHz, $CDCl_3$): δ 160.5, 160.0, 139.7, 138.7, 108.1, 105.6, 102.1, 100.8, 70.1 69.5, 33.6, 22.5, 10.5. MS (FAB) m/z 615.4 (M^+).

11-Br. The procedure above was followed using by 2.33 g (6.3 mmol) of **11** and 1.8 g (6.67 mmol) of PBr_3. The pure product was separated by silica column chromatography using 1:1 petroleum ether/CH_2Cl_2 as eluent affording 1.9 g (67%) of a white solid. ^{1}H NMR (270 MHz, $CDCl_3$): δ 7.67 (d, J = 8.37 Hz, 4H), 7.51 (d, J = 7.83 Hz, 4H), 6.62 (t, J = 2.16 Hz, 2H), 6.48 (bs, 1H), 5.09 (s, 4H), 4.39 (s, 2H). ^{13}C NMR (100 MHz, $CDCl_3$): δ 159.5, 141.9, 140.3, 132.5, 127.6, 118.6, 111.9, 108.3, 102.2, 69.0, 33.1. MS (FAB) m/z 433.1 (M^+).

12-Br. The procedure above was followed using 2.2 g (3.1 mmol) of **12** and 0.85 g (3.1 mmol) of PBr_3. The pure product was separated by silica column chromatography using 1:2 petroleum ether/CH_2Cl_2 as eluent affording 1.7 g (70%) of a white solid. ^{1}H NMR (270 MHz, $CDCl_3$): δ 8.13 (d, J = 8.37 Hz, 4H), 8.04 (d, J = 8.64 Hz, 4H), 7.57−7.51 (m, 8H), 6.65 (d, J = 2.16 Hz, 2H), 6.54 (t, J = 2.03 Hz, 1H), 5.10 (s, 4H), 4.41 (s, 2H), 1.35 (s, 18H). ^{13}C NMR (100 MHz, $CDCl_3$): δ 164.5, 163.9, 159.7, 155.3, 140.5, 139.6, 127.6, 127.1, 126.7, 126.0, 123.5, 120.9, 108.3, 102.1, 69.3, 35.0, 33.2, 31.0. MS (FAB) m/z 783.4 (M^+).

General Procedure for the PCC Oxidation. To a suspension of 1.5 equiv of PCC in CH_2Cl_2 was slowly added a solution of functionalized benzyl alcohol. After stirring for 1 h at room temperature, the reaction mixture was filtered through a silica gel column and the filtrate was evaporated to dryness. The crude product was then purified by silica column chromatography.

9-CHO. The above procedure was followed using 1 g (3.12 mmol) of **9** and 1 g (4.7 mmol) of PCC. The pure product was separated by silica column chromatography using CH_2Cl_2 as eluent affording 0.94 g (94.6%) of a white solid. ^{1}H NMR (270 MHz, $CDCl_3$): δ 9.88 (s, 1H), 7.43−7.32 (m, 10H), 7.09 (d, J = 2.43 Hz, 2H), 6.85 (t, J = 2.30 Hz, 1H), 5.08 (s, 4H). ^{13}C NMR (100 MHz, $CDCl_3$): δ 191.7, 160.2, 138.3, 136.1, 128.6, 128.1, 127.4, 108.5, 108.1, 70.2. MS (FAB) m/z 318.3 (M^+).

10-CHO. The above procedure was followed using 0.66 g (1.19 mmol) of **10** and 0.38 g (1.78 mmol) of PCC. The pure product was separated by silica column chromatography using 1:3 petroleum ether/CH_2Cl_2 as eluent affording 0.579 g (88.7%) of a colorless liquid. ^{1}H NMR (400 MHz, $CDCl_3$): δ 9.87 (s, 1H), 7.08 (d, J = 2.40 Hz, 2H), 6.84 (t, J = 2.40 Hz, 1H), 6.54 (d, J = 2.00 Hz, 4H), 6.41 (t, J = 2.40 Hz, 2H), 4.99 (s, 4H), 3.89 (t, J = 6.60 Hz, 8H), 1.83−1.67 (m, 8H), 1.02 (t, J = 7.40 Hz, 12H). ^{13}C NMR (100 MHz, $CDCl_3$): δ 191.8, 160.5, 160.3, 138.3, 138.3, 108.6, 108.2, 105.6, 100.8, 70.3, 69.5, 22.5, 10.5. MS (FAB) m/z 551.3 ($M^+ + 1$).

11-CHO. The above procedure was followed using 0.41 g (1.12 mmol) of **11** and 0.364 g (1.69 mmol) of PCC. The pure product was separated by silica column chromatography using CH_2Cl_2 as eluent affording 0.35 g (85.4%) of a white solid. ^{1}H NMR (270 MHz, $CDCl_3$): δ 9.89 (s, 1H), 7.69 (d, J = 8.10 Hz, 4H), 7.53 (d, J = 7.83 Hz, 4H), 7.09 (d, J = 2.43 Hz, 2H), 6.82 (t, J = 2.16 Hz, 1H), 5.15 (s, 4H). ^{13}C NMR (100 MHz, $CDCl_3$): δ 191.3, 159.9, 141.4, 138.6, 132.5. 127.6, 118.5, 112.0, 108.6, 108.4, 69.2. MS (FAB) m/z 368.4 (M^+).

12-CHO. The above procedure was followed using 0.4 mg (0.55 mmol) of **12** and 0.14 g (0.65 mol) of PCC. The pure product was separated by silica column chromatography using CH_2Cl_2 as eluent affording 0.3 g (78.5%) of a white solid. ^{1}H NMR (270 MHz, $CDCl_3$): δ 9.90 (s, 1H), 8.16 (d, J = 8.10 Hz, 4H), 8.05 (d, J = 8.1 Hz, 4H), 7.59 (d, J = 8.64 Hz, 4H), 7.54 (d, J = 8.10 Hz, 4H), 7.13 (d, J = 1.89 Hz, 2H), 6.89 (bs, 1H), 5.19 (s, 4H), 1.36 (s, 18H). ^{13}C NMR (67.8 MHz, $CDCl_3$): δ 191.2, 164.5, 163.8, 159.9, 155.2, 139.8, 138.4, 127.6, 127.0, 126.6, 125.9, 123.6, 120.8, 108.5, 108.3, 69.6, 35.1, 31.1. MS (FAB) m/z 719 (M^+).

13-CHO. The above procedure was followed using 2.1 g (2.7 mmol) of **13** and 0.8 g (3.7 mmol) of PCC. The pure product was separated by silica column chromatography using 1:1 petroleum ether/CH_2Cl_2 as eluent affording 1.65 g (78.8%) of a white solid. ^{1}H NMR (400 MHz, $CDCl_3$): δ 9.88 (s, 1H), 7.44−7.32 (m, 20H), 7.09 (d, J = 2.40 Hz, 2H), 6.84 (t, J = 2.20 Hz, 1H), 6.69 (d, J = 2.00 Hz, 4H), 6.60 (t, J = 2.40 Hz, 2H), 5.04 (s, 8H), 5.02 (s, 4H). ^{13}C NMR (100 MHz, $CDCl_3$): δ 191.8, 160.2, 160.1, 138.6, 138.3, 136.6, 128.6, 128.0, 127.5, 108.6, 108.3, 106.3, 101.6, 70.1, 70.0. MS (FAB) m/z 743.1 (M^+).

14-CHO. The above procedure was followed using 1.02 g (0.84 mmol) of **14** and 0.2 g (0.93 mmol) of PCC. The pure product was separated by silica column chromatography using 1:1 petroleum ether/CH_2Cl_2 as eluent affording 0.41 g (40.2%) of a colorless liquid. ^{1}H NMR (400 MHz, $CDCl_3$): δ 9.87 (s, 1H), 7.07 (d, J = 2.40 Hz, 2H), 6.84 (bs, 1H), 6.65 (d, J = 2.00 Hz, 4H), 6.56−6.55 (m, 2H), 5.54 (d, J = 2.00 Hz, 8H), 6.39 (bs, 4H), 5.00 (s, 4H), 4.94 (s, 8H), 3.88 (t, J = 6.60 Hz, 16H), 1.82−1.73 (m, 16H), 1.01 (t, J = 7.20 Hz, 24H). ^{13}C NMR (100 MHz, $CDCl_3$): δ 191.8, 160.5, 160.2, 160.1, 138.8, 138.5, 138.3, 108.6, 108.2, 106.3, 105.7, 101.7, 100.8, 70.2, 70.1, 69.5, 22.5, 10.5. MS (FAB) m/z 1207.3 (M^+).

15-CHO. The above procedure was followed using 0.3 g (0.36 mmol) of **15** and 0.085 g (0.39 mmol) of PCC. The pure product was separated by silica column chromatography using 1:1 petroleum ether/CH_2Cl_2 as eluent affording 0.26 g (84%) of a white solid. ^{1}H NMR (400 MHz, $CDCl_3$): δ 9.87 (s, 1H), 7.64 (d, J = 8.00 Hz, 8H), 7.50 (d, J = 8.40 Hz, 8H), 7.04 (d, J = 2.40 Hz, 2H), 6.75 (t, J = 2.20 Hz, 1H), 6.63 (d, J = 2.00 Hz, 4H), 6.51 (t, J = 2.00 Hz, 2H), 5.09 (s, 8H), 5.02 (s, 4H). ^{13}C NMR (100 MHz, $CDCl_3$): δ 191.6, 160.1, 159.6, 142.0, 139.0, 132.4, 128.6, 127.5, 118.6, 111.8, 108.6, 108.1, 106.5, 101.7, 69.9, 69.0. MS (FAB) m/z 843.0 (M^+).

16-CHO. The above procedure was followed using 0.65 g (0.42 mmol) of **16** and 0.1 g (0.46 mmol) of PCC. The pure product was separated by silica column chromatography using 1:1 petroleum ether/CH_2Cl_2 as eluent affording 0.584 g (90%) of a white solid. ^{1}H NMR (400 MHz, $CDCl_3$): δ 9.84 (s, 1H), 8.11 (d, J = 8.40 Hz, 8H), 8.03 (d, J = 8.80 Hz, 8H), 7.55 (d, J = 8.00 Hz, 8H), 7.52 (d, J = 8.40 Hz, 8H), 7.03 (d, J = 2.40 Hz, 2H), 6.78 (t, J = 2.40 Hz, 1H), 6.67 (d, J = 2.00 Hz, 4H), 6.57 (t, J = 2.00 Hz, 2H), 5.11 (s, 8H), 5.03 (s, 4H), 1.34 (s, 36H). ^{13}C NMR (100 MHz, $CDCl_3$): δ 191.5, 164.4, 163.8, 159.9, 159.7, 155.2, 140.3, 138.8, 138.2, 127.5, 126.9, 126.6, 125.9, 123.3, 120.7, 108.3, 108.1, 106.2, 101.5, 69.8, 69.1, 34.9, 30.9. MS (FAB) m/z 1544 (M^+).

General Procedure for the Wadsworth−Emmons Reaction. To a solution of 2:1 equiv of an aldehyde and bis(phosphonate) ester in anhydrous THF was slowly added 2.2 equiv of potassium *tert*-butoxide. After stirring for 16−24 h at room temperature, the solution mixture was quenched with water. The crude product was extracted twice with CH_2Cl_2, dried over anhydrous $MgSO_4$, and evaporated to dryness. The crude product was then purified by silica gel column chromatography.

1. The above procedure was followed using 278 mg (0.87 mmol) of aldehyde, 162 mg (0.427 mmol) of bis(phosphonate), and 177 mg (1.58 mmol) of potassium *tert*-butoxide. The pure product was separated by silica gel column chromatography using CH_2Cl_2 as eluent, affording 224 mg (75%) of a yellow solid. ^{1}H NMR (270 MHz, $CDCl_3$): δ 7.47 (s, 4H), 7.45−7.32 (m, 20H), 7.03 (s, 4H), 6.76 (d, J = 2.16 Hz, 4H), 6.54 (t, J = 2.16 Hz, 2H), 5.06 (s, 8H). ^{13}C NMR (100 MHz, $CDCl_3$): δ 160.2, 139.4, 136.8, 136.6, 128.8, 128.6, 128.5, 128.0, 127.6, 126.9, 105.8, 101.6, 70.1. MS (FAB) m/z 706.5 (M^+). Anal. Calcd for $C_{54}H_{38}O_4N_4$: C, 84.96; H, 5.99. Found: C, 84.85; H, 5.94. mp 120−123 °C; decomposition temperature 260 °C.

2. The above procedure was followed using 578 mg (1.05 mmol) of aldehyde, 200 mg (0.53 mmol) of bis(phosphonate), and 150 mg (1.33 mmol) of potassium *tert*-butoxide. The pure product was separated by silica gel column chromatography using CH_2Cl_2 as eluent affording 510 mg (82%) of a green solid. ^{1}H NMR (400 MHz, $CDCl_3$): δ 7.47 (s, 4H), 7.05 (d, J = 16.40 Hz, 2H), 7.01 (d, J = 16.40 Hz, 2H), 6.75 (d, J = 2.40 Hz, 4H), 6.57 (d, J = 2.40 Hz, 8H), 6.53 (t, J = 1.60 Hz, 2H), 6.41 (t, J = 2.00 Hz, 4H), 4.98 (s, 8H), 3.90 (t, J = 6.80 Hz, 16H), 1.83−

Scheme 1. Synthesis of Functionalized Benzyl Bromides[a]

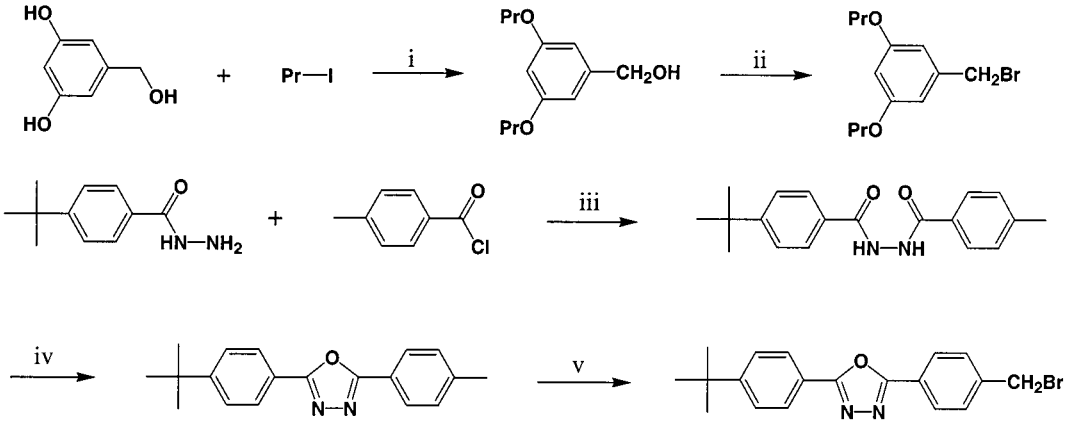

[a] Reagents and conditions: (i) K_2CO_3, 18-crown-6, acetone, 24 h, 91%; (ii) PBr_3, diethyl ether, overnight, 54%; (iii) Et_3N, $CHCl_3$, 90%; (iv) $POCl_3$, 90%; (v) NBS, benzoyl peroxide, CCl_4; 53%.

1.74 (m, 16H), 1.01 (t, J = 7.60 Hz, 24H). ^{13}C NMR (100 MHz, $CDCl_3$): δ 160.5, 160.1, 139.3, 139.0, 136.6, 136.0, 128.8, 128.5, 126.9, 105,7, 101.6, 100.8, 70.1, 69.6, 22.5, 10.5. MS (FAB) *m/z* 1171.8 (M^+). HRMS (MALDI-TOF): Calcd for $C_{74}H_{90}O_{12}$: 1170.6432. Found: 1170.6430 (M^+). mp 130−134 °C; decomposition temperature 250 °C.

3. The above procedure was followed using 193 mg (0.523 mmol) of aldehyde, 95 mg (0.251 mmol) of bis(phosphonate), and 110 mg (0.98 mmol) of potassium *tert*-butoxide. The pure product was separated by silica gel column chromatography using CH_2Cl_2 as eluent affording 132 mg (65%) of a yellow solid. ^{1}H NMR (270 MHz, $CDCl_3$): δ 7.68 (d, J = 8.37 Hz, 8H), 7.54 (d, J = 8.64 Hz, 8H), 7.47 (s, 4H), 7.03 (s, 4H), 6.75 (d, J = 1.89 Hz, 4H), 6.48 (s, 2H), 5.13 (s, 8H). ^{13}C NMR (100 MHz, $CDCl_3$): δ 159.7, 142.1, 139.8, 136.5, 132.5, 129.3, 128.2, 127.6, 127.0, 118.6, 111.9, 106.0, 101.6, 69.1. MS (FAB) *m/z* 806.4 (M^+). Anal. Calcd for $C_{54}H_{38}O_4N_4$: C, 79.77; H, 4.89; N, 7.15. Found: C, 79.79; H, 4.82; N, 7.00. mp 220−224 °C; decomposition temperature 300 °C.

4. The above procedure was followed using 313 mg (0.429 mmol) of aldehyde, 80 mg (0.211 mmol) of bis(phosphonate), and 79 mg (0.7 mmol) of potassium *tert*-butoxide. The pure product was separated by silica gel column chromatography using CH_2Cl_2 as eluent affording 200 mg (63%) of a yellow solid. ^{1}H NMR (400 MHz, $CDCl_3$): δ 8.15 (d, J = 8.40 Hz, 8H), 8.04 (d, J = 8.40 Hz, 8H), 7.60 (d, J = 8.00 Hz, 8H), 7.53 (d, J = 8.40 Hz, 8H), 7.48 (s, 4H), 7.07 (d, J = 16.40 Hz, 2H), 7.02 (d, J = 16.00 Hz, 2H), 6.78 (d, J = 1.60 Hz, 4H), 6.55 (bs, 2H), 5.16 (s, 8H), 1.35 (s, 36H).^{13}C NMR (100 MHz, $CDCl_3$): δ 164.7, 164.1, 159.9, 155.4, 140.7, 139.6, 136.5, 129.1, 128.3, 127.8, 127.2, 127.0, 126.8, 126.1, 123.6, 121.0, 106.0, 101.6, 69.4, 35.1, 31.1. HRMS (MALDI-TOF): Calcd for $C_{98}H_{90}O_8N_8$: 1506.6882. Found: 1507.6989 (M^++ 1). mp 138−141 °C; decomposition temperature 190 °C.

5. The above procedure was followed using 1.64 g (2.2 mmol) of aldehyde, 0.401 g (1.06 mmol) of bis(phosphonate), and 0.35 g (3.1 mmol) of potassium *tert*-butoxide. The pure product was separated by silica gel column chromatography using CH_2Cl_2 as eluent affording 1.41 g (85%) of a yellow solid. ^{1}H NMR (400 MHz, $CDCl_3$): δ 7.47 (s, 4H), 7.41−7.28 (m, 40H), 7.05 (d, J = 16.00 Hz, 2H), 7.01 (d, J = 16.40 Hz, 2H), 6.74 (d, J = 2.40 Hz, 4H), 6.69 (d, J = 2.00 Hz, 8H), 6.57 (t, J = 2.40 Hz, 4H), 6.51 (bs, 2H), 5.03 (s, 16H), 5.00 (s, 8H). ^{13}C NMR (100 MHz, $CDCl_3$): δ 160.1, 160.0, 139.3, 139.2, 136.7, 136.5, 128.8, 128.6, 128.5, 128.2, 128.0, 127.5, 126.9, 106.3, 105.8, 101.5, 70.0, 69.9. HRMS (MALDI-TOF): Calcd for $C_{106}H_{90}O_{12}$: 1554.6432. Found: 1554.6430 (M^+). mp 45−49 °C; decomposition temperature 275 °C.

6. The above procedure was followed using 408 mg (0.338 mmol) of aldehyde, 63 mg (0.167 mmol) of bis(phosphonate), and 50 mg (0.56 mmol) of potassium *tert*-butoxide. The pure product was separated by silica gel column chromatography using CH_2Cl_2 as eluent affording 297 mg (70%) of a yellow solid. ^{1}H NMR (400 MHz, $CDCl_3$): δ 7.49 (s, 4H), 7.06−7.05 (m, 4H), 6.77 (d, J = 2.00 Hz, 4H), 6.70 (d, J = 2.00 Hz, 8H), 6.56 (d, J = 2.40 Hz, 22H), 6.41 (m, 8H), 5.00 (s, 8H), 4.96 (s, 16H), 3.89 (t, J = 6.80 Hz, 32H), 1.82−1.74 (m, 32H), 1.01 (t, J = 7.60 Hz, 48H). ^{13}C NMR (100 MHz, $CDCl_3$): δ 160.4, 160.1, 160.0, 139.3, 139.1, 138.9, 136.5, 128.9, 128.4, 126.9, 106.6, 105.7, 101.5, 100.8, 100.8, 70.1, 70.0, 69.5, 22.5, 10.5. HRMS (MALDI-TOF): Calcd for $C_{154}H_{186}O_{28}NaK$: 2545.2665. Found: 2545.2670 (M^+ + Na + K). mp 45−49 °C; decomposition temperature 290 °C.

7. The above procedure was followed using 438 mg (0.52 mmol) of aldehyde, 82 mg (0.217 mmol) of bis(phosphonate), and 60 mg (0.53 mmol) of potassium *tert*-butoxide. The pure product was separated by silica gel column chromatography using CH_2Cl_2 as eluent affording 247 mg (65%) of a yellow solid. ^{1}H NMR (400 MHz, $CDCl_3$): δ 7.63 (d, J = 8.00 Hz, 16H), 7.49 (d, J = 8.00 Hz, 16H), 7.47 (s, 4H), 7.04 (d, J = 16.00 Hz, 2H), 7.00 (d, J = 16.00 Hz, 2H), 6.70 (d, J = 1.60 Hz, 4H), 6.64 (d, J = 2.00 Hz, 8H), 6.51 (bs, 4H), 6.40 (bs, 2H), 5.10 (s, 16H), 5.00 (s, 8H). **7** was too insoluble for ^{13}C NMR measurement. MS (FAB) *m/z* 1754.6 (M^+). HRMS (MALDI-TOF): Calcd for $C_{114}H_{90}O_{12}N_8$: 1754.6052. Found: 1754.6064 (M^+). mp 90−95 °C; decomposition temperature 262 °C.

8. The above procedure was followed using 550 mg (0.324 mmol) of aldehyde, 67 mg (0.177 mmol) of bis(phosphonate), and 50 mg (0.56 mmol) of potassium *tert*-butoxide. The pure product was separated by silica gel column chromatography using 1:1 CH_2Cl_2:EtOAc as eluent affording 210 mg (38%) of a yellow solid. ^{1}H NMR (400 MHz, $CDCl_3$): δ 8.10 (d, J = 8.00 Hz, 16H), 8.01 (d, J = 8.00 Hz, 16H), 7.55 (d, J = 8.40 Hz, 16H), 7.50 (d, J = 8.00 Hz, 16H), 7.39 (s, 4H), 6.96 (bs, 4H), 6.70 (bs, 10H), 6.57 (bs, 4H), 6.46 (bs, 2H), 5.12 (s, 16H), 5.02 (s, 8H), 1.33 (s, 72H). ^{13}C NMR (100 MHz, $CDCl_3$): δ 164.6, 164.0, 159.9, 159.8, 155.3, 140.5, 139.6, 139.4, 136.3, 128.8, 128.3, 127.7, 127.1, 126.9, 126.7, 126.0, 123.5, 120.9, 106.3, 105.7, 101.6, 101.6, 69.8, 69.4, 35.0, 31.1. HRMS (MALDI-TOF): Calcd for $C_{202}H_{180}N_{16}O_{20}$: 3149.3560. Found: 3149.3560 (M^+). mp 145−147 °C; decomposition temperature 200 °C.

Results and Discussion

The convergent approach[26] was employed to synthesize first-generation (G1) and second-generation (G2) poly(benzyl ether) type dendritic DSB bearing various functional moieties including propoxy, cyano, and 1,3,4-oxadiazole moieties on the outer surface or without bearing functional moiety. The preparation of the starting functionalized benzyl bromides is shown in Scheme 1 if the chemicals are not commercially available. Propylation of 3,5-dihydroxybenzyl alcohol with 1-iodopropane in the presence of K_2CO_3 and 18-crown-6 and then followed by bromination with PBr_3 afforded 3,5-dipropoxybenzyl bromide. 2-(4-*tert*-Butylphenyl)-5-[4-(bromomethyl)-phenyl]-1,3,4-oxadiazole was prepared

Scheme 2. General Scheme for the Synthesis of First- and Second-Generation Surface Functionalized Dendritic Distyrylstilbene[a]

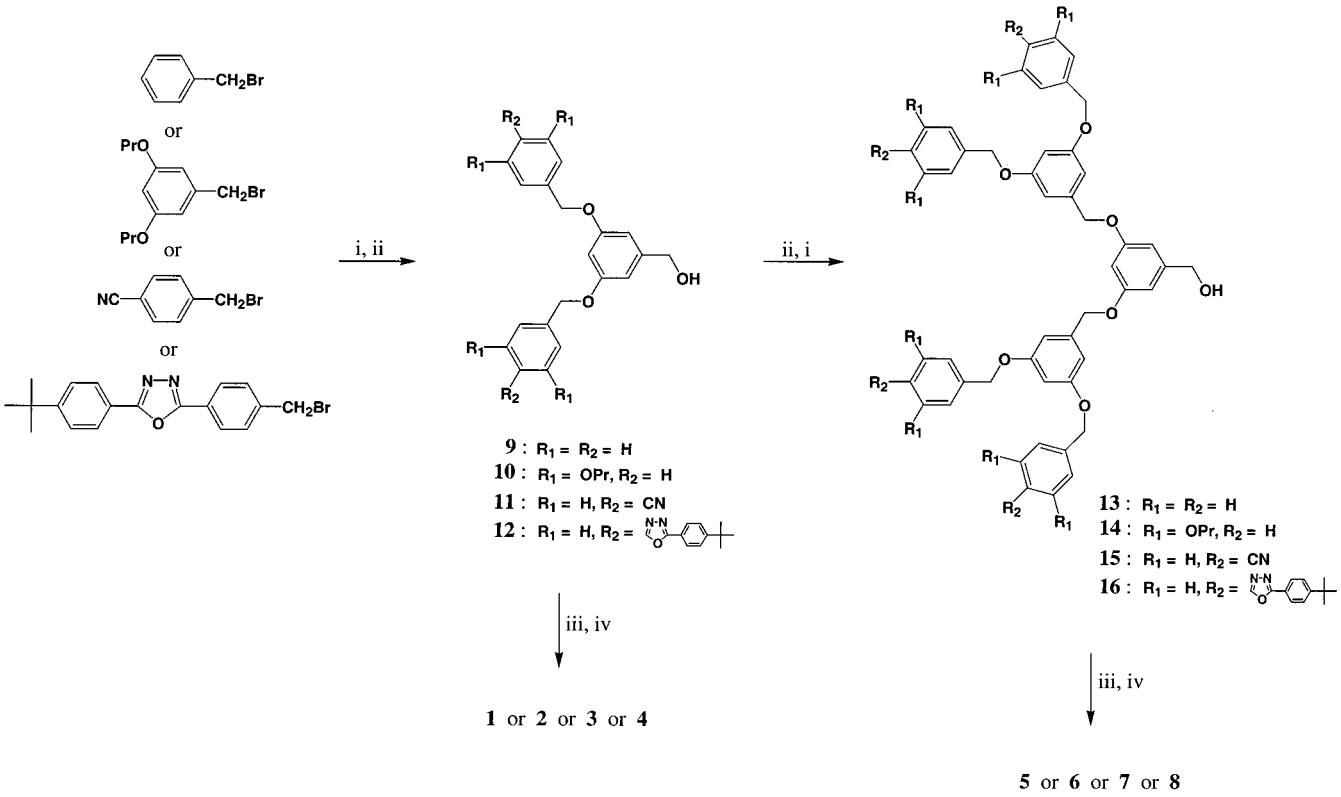

[a] Reagents and conditions: (i) 3,5-dihydroxybenzyl alcohol, K_2CO_3, 18-crown-6, acetone, 24−48 h (70−85%); (ii) PBr_3, diethyl ether, overnight (40−96%); (iii) PCC, CH_2Cl_2, 1 h (40−90%); (iv) bis(diethyl) *p*-xylylene(bis(phosphonate)), *t*-BuOK, 18-crown-6, THF, overnight (37−85%).

according to the following reaction sequence: acylation of 4-*tert*-butylbenzoic hydrazide with *p*-toluoyl chloride, followed by cyclodehydration of the acylated hydrazide in the presence of $POCl_3$ and finally free-radical bromination of 2-(4-*tert*-butylphenyl)-5-(4-methylphenyl)-1,3,4-oxadiazole. The general scheme for the synthesis of surface (un)functionalized dendritic DSB **1**−**8** is summarized in Scheme 2. The (un)functionalized G1 dendritic benzylic alcohols **9**−**12** were prepared by Williamson ether reaction of 3,5-dihydroxybenzyl alcohol with the corresponding functionalized benzyl bromide in the presence of K_2CO_3 and 18-crown-6. A subsequent reaction with PBr_3 afforded the (un)functionalized G1 dendritic benzylic bromide. An iterative Williamson ether reaction of 3,5-dihydroxybenzyl alcohol with the (un)functionalized G1 dendritic benzylic bromide afforded the corresponding (un)functionalized G2 dendritic benzylic alcohol **13**−**16**. PCC oxidation of the G1 or G2 dendritic benzylic alcohol gave the corresponding dendritic aldehyde. The double Wadsworth−Emmons reaction of the surface (un)functionalized G1 or G2 dendritic aldehyde with bis(phosphonate) ester in the presence of *t*-BuOK afforded the corresponding dendritic DSB **1**−**8**. All the new dendritic DSBs were fully characterized with standard spectroscopic techniques including ^{1}H NMR, ^{13}C NMR, and low/high-resolution mass spectroscopy (FAB or MALDI-TOF) or elemental analysis. All the dendritic DSBs are highly soluble in common organic solvents except cyano-functionalized series (**3** and **7**), which is only slightly soluble and were purified by column chromatography.

The aims of our theoretical calculations were not to accurately predict the properties of molecules but to understand and correlate the trends. As the calculations are based on the gas phase molecules, no attempt was made to compare the theoretical results directly with the experimental ones. The ground-state molecular geometries of G1 poly(benzyl ether) type dendritic DSB **1** and its methoxy-substituted derivative, analogue of **2**, and cyano-substituted derivative, **3**, were optimized by PM3 semiempirical methods in MOPAC 6. The results indicate that the surface (un)functionalized G1 poly(benzyl ether) type dendritic wedges attached at the ends of DSB core do not disrupt the coplanarity of the π-conjugated core in the PM3-optimized geometries. As also found from the properties calculations that although the poly(benzyl ether) type dendritic wedges are meta-linked at the nonconjugated positions of the π-conjugated DSB core, the HOMO and LUMO levels of these dendritic DSBs are perturbed as compared to that of the unsubstituted DSB (Table 1). The alkoxy substitution on the outer surface of dendritic wedges causes the destabilization of the HOMO and LUMO levels. On the other hand, the cyano substitution on the outer surface of dendritic wedges leads to the stabilization of the HOMO and LUMO levels. Such shifts are consistent with those substituted at para-conjugated positions of the DSB core, but the magnitudes are in a less extent.[27] It is interesting to find that the calculated HOMO−LUMO band gaps of these dendritic DSBs are essentially identical (Table 1). These results imply that the modifying of the surface functionalized dendritic wedges of an emissive dye can be used as a means to tune the HOMO and LUMO levels of the dye without greatly altering the HOMO−LUMO band gap. As the calculated energy gaps were determined for the gas phase, relaxation correction for solvent interaction would be needed when compared with those obtained

Table 2. Summaries of Physical Measurements of Dendritic DSBs 1−8

	λ_{max}[a]/nm ($\epsilon_{max}/10^{-4}$ M^{-1} cm^{-1})	λ_{den}[a]/nm ($\epsilon_{den}/10^{-4}$ M^{-1} cm^{-1})	emission band maxima[a]/nm	energy transfer efficiency[b]/%	FL quantum yield[c]
1	362 (5.93)		398, 421		0.98
2	362 (6.45)	285 (1.96)	398, 420	47.9	0.97
3	362 (5.71)		398, 421		0.95
4	362 (5.01)	294 (10.3)	398, 421	59	0.99
5	362 (5.89)	284 (1.86)	398, 419	43.5	0.98
6	362 (6.17)	283 (3.83)	398, 421	32.5	0.93
7	362 (5.71)	280 (3.19)	399, 421	17.5	0.97
8	362 (5.28)	293 (20.1)	400, 421	53	0.95

[a] Measured in $CHCl_3$. [b] Determined by comparing the absorption maximum of dendritic wedges of the absorption and fluorescence excitation spectra. [c] Determined by dilution method.

from the solution measurements.[22,23] The corrected energy gaps (see Table 1) are in good agreement with the optical band gaps determined from solution measurements.

In view of the electronic absorption spectra, all dendritic DSBs show very similar spectral features, which are basically composed of two major absorption bands (Table 2). The absorption appears around 280−294 nm due to the surface (un)functionalized poly(benzyl ether) type dendritic wedges and the absorption contributed from the DSB core peaks at 362 nm, which remains constant among various surface (un)functionalized dendritic wedges. The benzyl ether based surface (un)functionalized dendritic wedges generally exhibit only weak absorbance as compared to that of the core, but the wedge absorption increases as the wedge generation increases. However, it is important to note that oxadiazole-substituted dendritic wedges show much stronger absorbance (2−4 times) than the DSB core. There are also no apparent differences in the absorption characteristics including absorption maximum of the DSB core as the dendrimer generation increases. The absorption bands of all dendritic DSB cores show clear vibronic fine structures, indicating planarity and restricted rotation of the π-conjugated backbone as predicted by the PM3 semiempirical calculations. On the other hand, their absorption maxima are slightly red-shifted (Δ6 nm) as compared to that of the unsubstituted DSB (Table 2).

Model studies on emission properties of the surface (un)functionalized dendritic wedges showed that only oxadiazole-substituted dendritic wedges exhibit fluorescence emission (i.e., **12** at 341/358 nm and **16** at 344/357 nm), and all other G1 and G2 surface (un)-functionalized dendritic wedges do not fluoresce. The emission spectra of all the G1 and G2 dendritic DSBs are apparently identical with blue-light emission bands at 398 and 421 nm in solution when excited at 362 nm (λ_{max} of core) (Table 2). For oxadiazole-substituted dendrimers **4** and **8**, when excitation was carried out at the oxadiazole-substituted dendritic wedges, very strong emission associated with the DSB core was mainly resulted. This core emission intensity is even greater than that obtained from direct excitation of the core. This clearly indicates that the energy is transferred from the oxadiazole-substituted dendritic wedges to the core. Even though other surface (un)functionalized dendritic wedges do not fluoresce, excitation of the dendritic wedges of this class of dendrimers (**1**−**3** and **5**−**7**) also results in core emission. The emission intensity is proportional to the extinction coefficient of the excitation wavelength. This again indicates that the energy transfer interaction takes place in these surface (un)functionalized dendritic DSBs. It has been shown

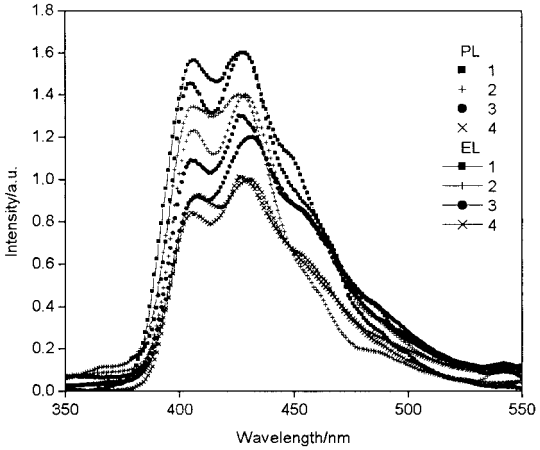

Figure 1. Normalized photoluminescence and electroluminescence spectra of first-generation dendritic DSBs **1**−**4** doped in PVK thin film. For clarity, each set of spectra is offset.

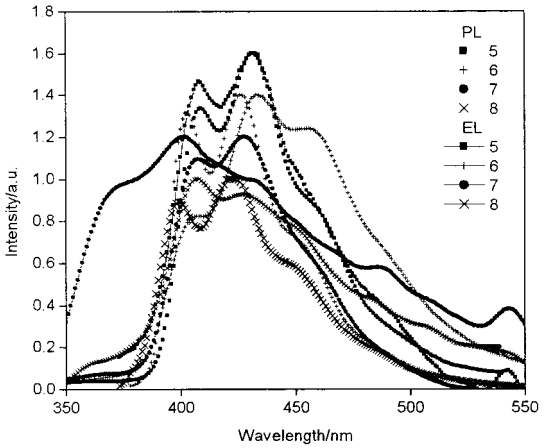

Figure 2. Normalized photoluminescence and electroluminescence spectra of first-generation dendritic DSBs **5**−**8** doped in PVK thin film. For clarity, each set of spectra is offset.

that efficient energy transfer from fifth-generation polybenzyl ether type dendritic wedges to the porphyrin core occurred efficiently in the tetrasubstituted porphyrin dendrimer.[28] To evaluate the energy transfer efficiency of the dendritic DSB, we compared the difference in intensity at the absorption maximum of dendritic wedges of the absorption spectrum and the fluorescence excitation spectrum recorded at the emission of the core of the corresponding dendrimer.[29] The results were tabulated in Table 2. The energy transfer from the surface (un)functionalized dendritic wedges to the core is fairly substantial in most of the cases. It appears that G1 surface functionalized dendritic wedges are more efficient in funneling energy to the core than those of the G2 generation. Importantly, all dendritic DSBs

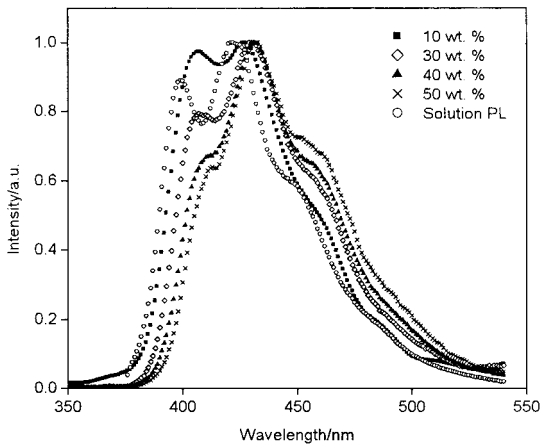

Figure 3. Concentration dependence of photoluminescence spectra of **8** doped thin film.

exhibit very high fluorescence quantum yields (over 93%). Such a high fluorescence quantum yield in these dendritic DBSs is attributed to the rigidity and coplanarity of the π-conjugated skeleton isolated by the dendritic wedges. The thermal gravimetric analysis indicates that all dendritic DSBs show good thermal stabilities with decomposition temperature in the range 190−300 °C. With all these desired physical properties, this class of dendritic DSBs may be potentially useful for light emitting applications.

The solid-state photoluminescence (PL) spectra were measured from dendritic DSB doped poly(*N*-vinylcarbazole) (PVK) film as shown in Figures 1 and 2. The spectral features of the thin-film PL spectra are often concentration dependent as shown in Figure 3. In a low DSB doping concentration, the spectral features are very similar to those of the corresponding dendritic DSB in solution. But in a high doping level, the emission maxima are slightly red-shifted ($\Delta\lambda_{em} = 9$ nm for 50 wt % of **8**), and the emission bands are broadened with variation in vibronic intensities, which are attributed to an increase in the intermolecular interaction of the dendritic DSBs. Nevertheless, the spectral features suggest that the PL emissions of the doped films arise from dendritic DSBs but not from PVK polymer. Single-layer OLEDs using dendritic DSB doped poly(*N*-vinylcarbazole) (PVK) film as an emissive layer with structure of (ITO/DSB:PVK/Al) were fabricated and investigated. Consistently, the emission wavelengths and spectral features of the EL spectra are very similar to those of the corresponding solid-state PL spectra (Figures 1 and 2). These also suggest that their EL emissions originate from dendritic DSBs. In general, there is an initial increase in light emission intensity with an increase in dendritic DSB content, but the intensity becomes saturated and then decreases at a high doping level. In the structure−properties investigation, the dendritic DSB content in the doped film was kept constant (at 0.133 mmol of dendritic DSB per gram of PVK) for easy comparison. For the G1 dendritic DSB based single-layer devices, the turn-on voltage for both current and light are similar, indicating a fairly balanced charge injection and transport (Figure 4). However, it is not the case for the G2 dendritic DSB based devices, and their turn-on voltages were generally a few volts higher than those of the corresponding G1 dendritic DSB based devices (Figure 5). Such adverse effects for G2 based devices are presumably due to an effective shielding of G2 dendritic wedges, which deteriorates the charge transport properties of the dendrimer.[30] However, the external quantum efficiency of the second-generation dendritic DSB based single-layer LED, which was calculated from the measured EL intensity divided by the current density passing through the device, is found to be higher than that of the corresponding first-generation dendrimer based devices (Figures 4 and 5). In addition, the cyano surface functionalized dendritic DSB based LEDs exhibit poor device performance and relative stability, which are likely due to the aggregate

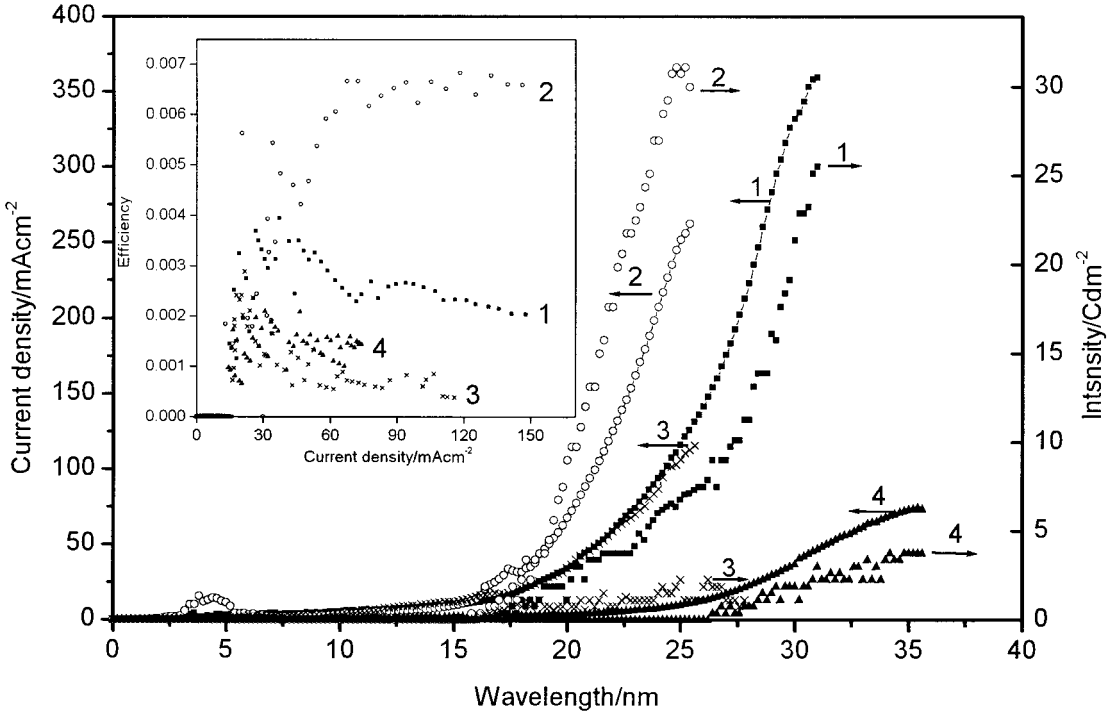

Figure 4. Current−voltage and light−voltage characteristics of first-generation dendritic DSBs **1**−**4** doped single-layer LEDs with structure of (ITO/DSB:PVK/Al). The inset is the curves of external efficiencies over current densities.

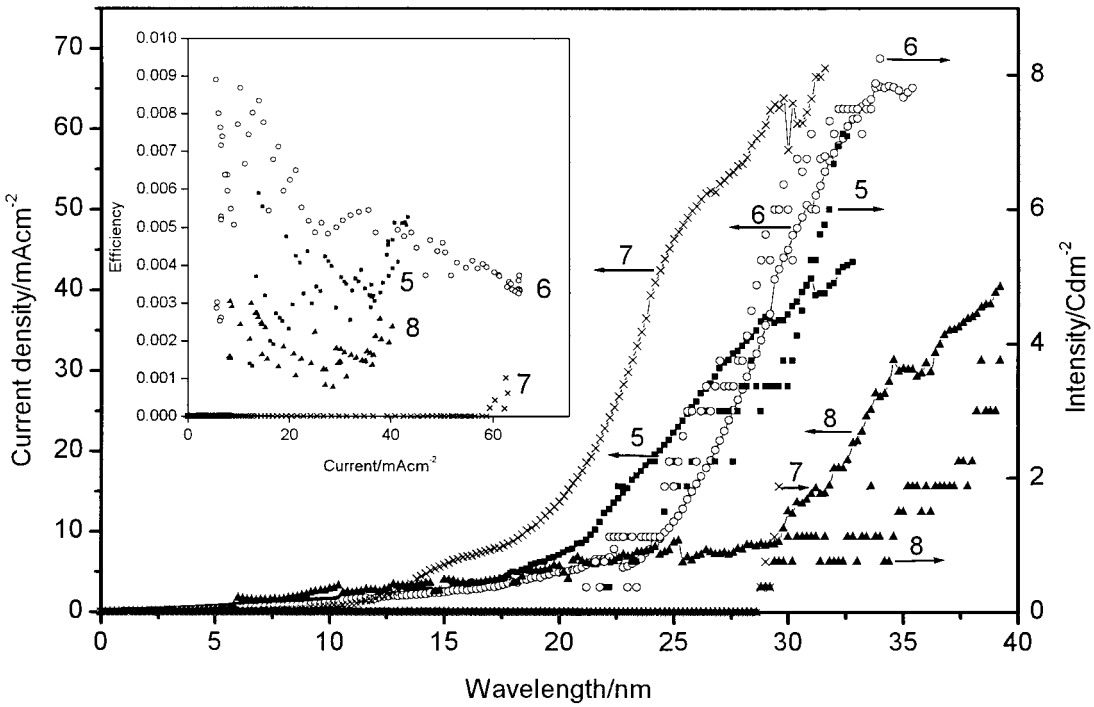

Figure 5. Current−voltage and light−voltage characteristics of first-generation dendritic DSBs **5** and **6** doped single-layer LEDs with structure of (ITO/DSB:PVK/Al). The inset is the curves of external efficiencies over current densities.

formation of these slightly soluble dye. On the other hand, the propoxy surface functionalized dendritic DSB based devices consistently exhibit the best external quantum efficiency and relative stability among the others. As a result, the propoxy surface functionalized dendritic DSB shows potential for further development. No attempt was made to optimize the device performance in the present studies even though device performance can be enhanced by various means such as using low-resistance ITO glass and low-work function cathode.

In summary, we have successfully synthesized a novel series of surface functionalized poly(benzyl ether) type dendritic distyrylbenzenes bearing various electron or hole affinitive moieties on the outer surface of the first- and second-generation dendritic wedges for blue-light emission. Incorporation of the G1 or G2 surface functionalized dendritic wedges at the ends of distyrylbenzene does not cause disruption of the π-conjugation of the core. Although the surface functionalized dendritic wedges do not alter the optical band gap of the distyrylbenzene core, the HOMO and LUMO levels of the core are perturbed according to the electronic nature of the surface functional groups. Excitation of the surface functionalized dendritic wedges results in substantial energy transfer to the emissive core even though the surface functionalized dendritic wedges themselves fluoresce weakly or do not fluoresce. In addition, all the dendritic distyrylstilbenes show very high fluorescence quantum yields (over 93%). In addition, single-layer light emitting diodes (LED) using dendritic distyrylstilbenes (DSB) doped poly(*N*-vinylcarbazole) (PVK) film as an emissive layer with structure of (ITO/DSB:PVK/Al) have been fabricated and investigated. The emission wavelengths and spectral features of dye doped solid-state photoluminescence and electroluminescence at a low doping concentration are very similar to those of the solution emission. Although the external quantum efficiency of the second-generation dendritic DSB based single-layer LED is higher than that of the corresponding first-generation dendrimer based devices, the overall device performance is inferior. On the other hand, the propoxy surface functionalized dendritic DSB devices consistently show the best device performance and relative stability among the others.

Acknowledgment. This work was supported by Faculty Research Grants (FRG/99-00/II-11) and (FRG/99-00/I-04) from Hong Kong Baptist University. We gratefully acknowledge Dr. Y. Tao at NRC, Canada, for the MALDI-TOF mass spectroscopy measurements and Dr. S. K. So at HKBU for the access of his research facility to perform the EL experiments.

References and Notes

(1) Tang, C. W.; VanSlyke, S. A. *Appl. Phys. Lett.* **1987**, *52*, 913−915.
(2) Burroughes, J. H.; Bradley, D. D. C.; Brown, A. R.; Marks, R. N.; Mackay, K.; Friend, R. H.; Burn, P. L.; Holmes, A. B. *Nature* **1990**, *347*, 539−541.
(3) Friend, R. H.; Gymer, R. W.; Holmes, A. B.; Burroughes, J. H.; Marks, R. N.; Taliani, C.; Bradley, D. D. C.; Dos Santos, D. A.; Brédas, J. L.; Lögdlund, M.; Salaneck, W. R. *Nature* **1999**, *397*, 121−128.
(4) Kraft, A.; Grimsdale, A. C.; Holmes, A. B. *Angew. Chem., Int. Ed.* **1998**, *37*, 402−428.
(5) Mitschke, U.; Bäuerle, P. *J. Mater. Chem.* **2000**, *10*, 1471−1507.
(6) Greenham, N. C.; Moratti, S. C.; Bradley, D. D. C.; Friend, R. H.; Holmes, A. B. *Nature* **1993**, *365*, 628−630.
(7) Brown, A. R.; Bradley, D. D. C.; Burroughes, J. H.; Friend, R. H.; Greenham, N. C.; Burn, P. L.; Holmes, A. B. *Appl. Phys. Lett.* **1992**, *61*, 2793−2795.
(8) Segura, J. L.; Martin, N. *J. Mater. Chem.* **2000**, *10*, 2403−2453.
(9) Müllen, K.; Wegner, G. *Electronic Materials: The Oligomer Approach*; Wiley-VCH: Weinheim, 1998.
(10) Newkome, G. R.; Moorefield, C. N.; Vögtle, F. *Dendritic Molecules: Concept, Synthesis, Perspectives*; VCH: Weinheim, 1996.
(11) Fréchet, J. M. J.; Hawker, C. J. In *Comprehensive Polymer Science*, 2nd Suppl.; Aggarwal, S. L., Russo, S., Eds.; Pergamon: Oxford, 1996; pp 140−206.

(12) Matthews, O. A.; Shipway, A. N.; Stoddart, J. F. *Prog. Polym. Sci.* **1998**, *23*, 1−56.
(13) Frey, H.; Lach, C.; Lorenz, K. *Adv. Mater.* **1998**, *10*, 279−293.
(14) Fischer, M.; Vögtle, F. *Angew. Chem., Int. Ed.* **1999**, *38*, 885−905.
(15) Bosman, A. W.; Jansen, H. M.; Meijer, E. W. *Chem. Rev.* **1999**, *99*, 1665−1688.
(16) Majoral, J. P.; Caminade, A. M. *Chem. Rev.* **1999**, *99*, 845−880.
(17) Adronov, A.; Fréchet, J. M. J. *Chem. Commun.* **2000**, 1701−1710.
(18) Kraft, A. *J. Chem. Soc., Chem. Commun.* **1996**, 77−79.
(19) Wang, P. W.; Liu, Y. J.; Devadoss, C.; Bharathi, P.; Moore, J. S. *Adv. Mater.* **1996**, *8*, 237−241.
(20) Halim, M.; Pillow, J. N. G.; Samuel, I. D. W.; Burn, P. L. *Adv. Mater.* **1999**, *11*, 371−374.
(21) Freeman, A. W.; Koene, S. C.; Malenfant, P. R. L.; Thompson, M. E.; Fréchet, J. M. J. *J. Am. Chem. Soc.* **2000**, *122*, 12385−12386.
(22) Sato, N.; Seki, K.; Inokuchi, H. *J. Chem. Soc., Faraday Trans. 2* **1982**, *77*, 1621−1633.
(23) Mitschke, U.; Osteritz, E. M.; Debaerdemaeher, T.; Sokolowski, M.; Baeuerle, P. *Chem. Eur. J.* **1998**, *4*, 2211−2224.
(24) Parker, C. A.; Rees, W. T. *Analyst* **1960**, *85*, 587−589.
(25) Peng, Z.; Bao, Z.; Galvin, M. E. *Adv. Mater.* **1998**, *10*, 680−684.
(26) Hawker, C. J.; Fréchet, J. M. J. *J. Am. Chem. Soc.* **1990**, *112*, 7638−7647.
(27) Wong, M. S.; Li, Z. H.; Shek, M. F.; Chow, K. H.; Tao, Y.; D'Iorio, M. *J. Mater. Chem.* **2000**, *10*, 1805−1810.
(28) Jiang, D. L.; Aida, T. *J. Am. Chem. Soc.* **1998**, *120*, 10895−10901.
(29) Stryer, L.; Haugland, R. P. *Proc. Natl. Acad. Sci. U.S.A.* **1967**, *58*, 719−726.
(30) Lupton, J. M.; Samuel, I. D. W.; Beavington, R.; Burn, P. L.; Bässler, H. *Adv. Mater.* **2001**, *13*, 258−260.

MA010749+